Jansky-Bielschowsky Variant Disease: CT, MRI, and SPECT Findings

Taina Autti, MD*, Raili Raininko, MD, PhD†, Jyrki Launes, MD†, Auli Nuutila, MD‡, and Pirkko Santavuori, MD, PhD*

Six patients with a variant type of Jansky-Bielschowsky (JBVD) disease were examined using 3 different imaging methods. Five of the patients underwent computed tomography, 4 magnetic resonance imaging, and 5 single photon emission computed tomography. All patients had brain atrophy that was most severe in the cerebellum. Magnetic resonance imaging demonstrated the parenchymal abnormalities well; all patients had hyperintense periventricular white matter, especially around the bodies and atria of the lateral ventricles, and a significant decrease in signal intensity in the thalami and/or putamina. Single photon emission computed tomography disclosed hypoperfusion of the cerebellum in all patients. Neuroimaging examinations are valuable in the diagnosis of JBVD. It may be difficult to divide patients with neuronal ceroid-lipofuscinosis disorders into clinical subtypes in the early stage of the disease. Magnetic resonance imaging, especially when combined with a typical clinical pattern, makes the diagnosis of JBVD highly likely. Radiologic examinations of the brain may also prove important in following the progression, as well as in investigating the pathophysiology, of the disease.

Autti T, Raininko R, Launes J, Nuutila A, Santavuori P. Jansky-Bielschowsky variant disease: CT, MRI, and SPECT findings. Pediatr Neurol 1992;8:121-6.

Introduction

Jansky-Bielschowsky disease is a progressive encephalopathy initially described by Jansky [1] and Bielschowsky [2] and later defined as a late infantile type of neuronal ceroid-lipofuscinosis (NCL) [3] because the neural and visceral cells accumulate large amounts of material evidencing positive histochemical reactions of ceroid and lipofuscin. Recently, it was determined that a major proportion of the stored material is composed of proteins and it was suggested that NCL disorders are proteolipid proteinoses [4].

Late infantile NCL usually begins at the age of 2-4 years with epilepsy as the leading symptom soon followed by mental retardation, ataxia, myoclonia, and visual failure. The disease is known to occur worldwide [6,7]. Variant Jansky-Bielschowsky disease, however, may have a more delayed age of onset and/or other features that distinguish it from the classic type [8-10].

The diagnosis of classic Jansky-Bielschowsky disease is confirmed relatively easily because the characteristic neurophysiologic findings appear during an early stage [11]. In the variant type, conversely, giant visual evoked potentials (VEPs), somatosensory evoked potentials (SEPs), and typical EEG signs (i.e., spikes evoked by a low rate of photic stimulation) appear for the first time several years after the onset of the clinical symptoms [9]; therefore, other diagnostic tools are needed during the beginning stages of the disorder.

We report our findings from computed tomography (CT), magnetic resonance imaging (MRI), and single photon emission computed tomography (SPECT) of the brain in variant Jansky-Bielschowsky disease (JBVD) and emphasize their use in the diagnosis.

Methods

Patients and Clinical Data. The study consisted of 6 patients (3 boys, 3 girls). In all patients early psychomotor development was normal. The first signs of the disease were usually slight mental retardation and motor clumsiness observed in all patients between 4-7 years of age. Ataxia, myoclonia, slight dysarthria, and epilepsy developed between 8 and 10 years of age. Mental retardation progressed rapidly and by the age of 9 years none had IQ scores over 66. No vacuolated lymphocytes were found and all routine laboratory tests were normal. All children had macular and retinal degeneration and slight optic atrophy. The electroretinogram became undetectable at ages 8-9½ years.

Ultrastructural studies revealed cytosomes with fingerprint profiles in autonomic ganglion cells and with both fingerprint and curvilinear profiles in extraneural cells. A characteristic neurophysiologic triad developed between 7½ and 10½ years of age: high SEP at the age of 7½-9½ years, high VEP at 8-9½ years, and photic spikes on EEG at 8½-10½ years.

Radiologic Examinations

CT. Five patients underwent a CT examination at ages 6-10 years, 1-3½ years after the clinical onset of the disease. One girl underwent

From the *Department of Child Neurology; University of Helsinki; †Department of Diagnostic Radiology and Central Laboratory; University Central Hospital; Helsinki, Finland; ‡Department of Paediatrics; Central Hospital of Seinäjoki; Seinäjoki, Finland.

Communications should be addressed to:
Dr. Autti; Department of Child Neurology; Children's Hospital; University of Helsinki; SF-00290 Helsinki, Finland.
Received August 20, 1991; accepted December 18, 1991.

Table 1. CT findings

Patient No./Sex/ Age (yrs)	Time Elapsed from Clinical Onset (yrs)	Infratentorial Regions	Supratentorial Regions
1/M/6	1	IVth ventricle dilated, cerebellar sulci enlarged, ambient cisterns enlarged	—
2/F/7	1	IVth ventricle dilated, cerebellar sulci severely enlarged	IIIrd ventricle quite large but still within normal range, temporal horns slightly dilated, cerebral sulci and sylvian fissures enlarged
3/M/8	3½	IVth ventricle dilated, cerebellar hemispheres atrophic	Tips of temporal horns slightly dilated
4/F/8*	1	IVth ventricle dilated, ambient cisterns slightly enlarged	—
4/F/10†	3	IVth ventricle more enlarged, ambient cisterns more enlarged, size of vermis reduced	IIIrd ventricle larger than on 1st examination, temporal horns larger, sylvian fissures larger
5/F/9	3	IVth ventricle dilated, cerebellum atrophic	Tips of temporal horns quite large but within normal range, some cerebral sulci slightly enlarged

* First examination.
† Second examination.

the examination twice, at the ages of 8 and 10 years. CT scans were performed with routine protocols without contrast enhancement.

MRI. Four patients (2 boys, 2 girls) underwent MRI at ages 6-11 years, a few months to 4 years after the clinical onset of the disease. The examinations were performed with a Siemens Magnetom imager operating at 1.0 T. T_1-weighted sagittal slices with gradient echo sequences and axial slices with a sequence SE 2500/22-90 ms were obtained in all examinations and in 2 patients coronal slices also were obtained with the SE sequence. Slice thickness was 5 mm and matrix size 256 × 256. Fifteen children who were either healthy or who had no disease affecting the brain formed the control group. T_1-weighted sagittal slices and T_2- and proton-density-weighted images, and intensity ratios between structures were calculated. Distilled water was used as a reference. Any value was considered pathologic if it differed from the controls by more than 2 S.D. The size of some anatomic structures was also measured from proton-density-weighted images at several locations in each lobe. Statistical analyses were performed using 2-tailed *t* tests.

SPECT. Five patients (2 boys, 3 girls) underwent SPECT at ages 6-9 years, a few months to 7 years after the clinical onset of the disease. The examinations were performed with a GE 400T large field-of-view rotating gamma camera equipped with a low-energy parallel hole collimator. After an intravenous injection of technetium-99m hexamethylpropyleneamineoxime (^{99m}Tc-HmPAO; 6.0-14.5 mCi), 64 frames (1 frame per 30 s) were collected. Transversal, coronal, and sagittal slices of 14 mm thickness were produced using the Gamma-11 software's filtered back-projection algorithm and the modified Shepp-Logan filter. The images were printed using a 16-color scale. Perfusion in the cerebellar hemispheres and in each cerebral lobe were scored visually.

Results

CT and MRI Findings. The CT and MRI findings in each patient are summarized in Tables 1 and 2.

All but 1 patient had an enlarged fourth ventricle and in all but one examination atrophic changes were found in the cerebellar hemispheres or vermis (Fig 1). The size of the brainstem is better demonstrated by MRI than by CT; brainstem atrophy was established in every patient examined using MRI. Supratentorial atrophy was not so pronounced, but enlargement of the tips of the temporal horns was found in every patient.

Patients 1 and 2 were examined twice and Patient 4, 3 times; in all of them, atrophic changes demonstrated progression. Although ventricles, cisterns, fissures, or sulci still were within the normal range during the latter examination, the volumes of these structures had increased.

CT did not reveal pathologic attenuation in the brain parenchyma, whereas MRI disclosed parenchymal abnormalities in all patients examined. All patients had hyperintense periventricular white matter, especially around the bodies and atria of the lateral ventricles in both T_2- and proton-density-weighted images (Figs 2A,2B). In every patient, a significant decrease in signal intensity was found in the thalami and/or putamina in T_2-weighted images (Fig

Table 2. MRI findings

Patient No./Sex/ Age (yrs)	Time Elapsed from Clinical Onset	Atrophic Changes	Intensity Changes
6/M/6	Few months	Brainstem reduced in size, cerebellar sulci slightly enlarged, temporal horns of lateral ventricles slightly dilated, cerebral sulci slightly enlarged	Hyperintense zones in white matter around lateral ventricles, intensity loss in thalami and posteriorly in putamina, posterior limbs of internal capsules slightly hyperintense
1/M/9	4 yrs	All ventricles dilated, brainstem reduced in size, atrophy of cerebellum, cerebral sulci enlarged	Hyperintense zones in white matter around lateral ventricles, intensity loss in thalami and putamina
2/F/10	4 yrs	All ventricles dilated, brainstem reduced in size, atrophy of cerebellum, abnormally thick CSF layer over convexity, cerebral sulci markedly enlarged	Hyperintense zones in white matter around lateral ventricles, intensity loss in putamina on T_2-weighted images and in thalami on proton-density-weighted images
4/F/11	4 yrs	IIIrd and IVth ventricles dilated, brainstem reduced in size, vermis reduced in size, cerebellar sulci slightly enlarged, sylvian fissures and some cerebellar sulci enlarged	Hyperintense zones in white matter around lateral ventricles, intensity loss in thalami

2C). In proton-density-weighted images, signal loss was more pronounced in the thalami. In one patient, the heads of the caudate nuclei also had a hypointense appearance upon visual evaluation of both T_2- and proton-density-weighted images, but the values calculated from the T_2-weighted images did not differ significantly from the values obtained for the controls.

The corpus callosum was thinner in the patients than in the controls ($P < .01$). The cortex was significantly thinner in the patients than in the controls in the frontal and occipital lobes ($P < .001$) but not in the parietal lobes ($P < .05$).

SPECT Findings. The SPECT findings in each patient are summarized in Table 3. All patients had moderate or severe cerebellar hypoperfusion. The hypoperfusion was severe in all patients examined 3-7 years after the clinical onset of the disease. In the patient examined only a few months after the clinical onset, the hypoperfusion of the cerebellum was moderate. Focal cerebral, unilateral, or bilateral perfusion abnormalities were also found in at least the temporal regions of all patients.

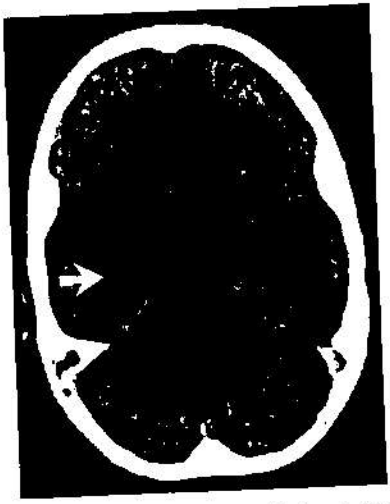

Figure 1. Cranial CT of a 7-year-old girl demonstrating dilated fourth ventricle and severely enlarged cerebellar sulci. The tips of the temporal horns (arrow) are slightly dilated.

Discussion

Santavuori et al. recently drew attention to the wide spectrum of Jansky-Bielschowsky disease [9]. In their report, some CT and SPECT findings were included, but detailed data were not provided and the role of neuroradiologic studies was not discussed.

The typical CT finding observed in all patients in the present series was severe atrophy in the posterior fossa combined with mild supratentorial atrophy. Although atrophic changes have been reported in many encephalopathies, the prominence of the atrophy in the posterior fossa is rather unusual, but it has also been found in classic Jansky-Bielschowsky disease [12,13]. Nonspecific atrophic changes were found in a few other reports of classic Jansky-Bielschowsky disease [14-16].

In our study, MRI demonstrated white matter abnormalities in all patients. Periventricular white matter was hyperintense, especially around the bodies and atria of the lateral ventricles. In every patient a significant decrease in signal intensity in the thalami and/or putamina was found. The corpus callosum was thin and the frontal and occipital

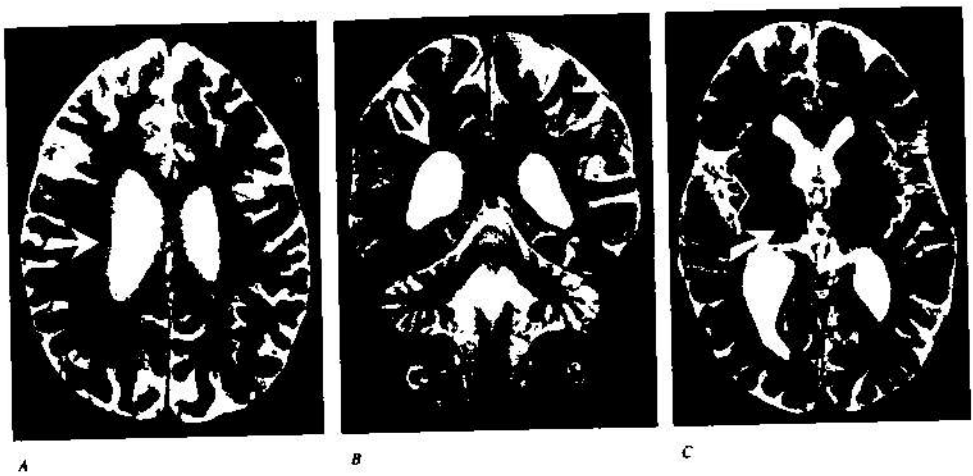

Figure 2. MRI obtained from a 9-year-old boy. (A,B) Hyperintensities (arrows) in the white matter around the dilated lateral ventricles: (A) transversal slice and (B) coronal slice. (C) Decreased signal intensity in the thalami (white arrow) and posterior putamina (open arrow). Heads of the caudate nuclei have a normal signal intensity (black arrow). The third and lateral ventricles are dilated. (B) Cerebellar and (A-C) cerebral sulci are enlarged.

cortex was thinner than normal. These changes are also nonspecific and have been found in many encephalopathies of children and adults [17-19].

SPECT revealed moderate or severe hypoperfusion in the cerebellum which correlated well with the cerebellar atrophy and the clinical picture. Focal cerebral hypoperfusion was also found in areas where no obvious atrophy was observed on CT or MRI. Focal hypoperfusion on SPECT without atrophic changes has also been observed in other encephalopathies. It seems that the functional and anatomic changes do not appear simultaneously in neurodegenerative disorders.

Although they appear to be nonspecific, CT and MRI findings in JBVD can be utilized in the differential diagnosis. It may be difficult to divide NCL patients into clinical subtypes during the early stage of the disease. This is particularly true in the Jansky-Bielschowsky disease with its many clinical variations [9]. In our series of 6 children, one child (Patient 6) was examined with MRI soon after the first symptoms. This 6-year-old boy had typical white matter intensity changes, but the atrophic changes in the cerebellum were not as prominent as in older patients with JBVD. The neurophysiologic findings were normal except for the ERG and EEG. ERG was undetectable and EEG

Table 3. SPECT findings

Patient No./Sex/ Age (yrs)	Time Elapsed from Clinical Onset	Hypoperfusion in Infratentorial Regions	Hypoperfusion in Supratentorial Regions
1/M/8	3 yrs	Cerebellar	Bilateral temporal, R frontal
2/F/10	4 yrs	Cerebellar	Bilateral occipital, L temporal, L parietal
4/F/10	3 yrs	Cerebellar	Bilateral occipital, bilateral temporal
5/F/13	7 yrs	Cerebellar	Slight R temporal, slight R parietal, slight R frontal
6/M/6	Few months	Cerebellar	Bilateral temporal

Abbreviations:
L = Left
R = Right

was abnormal, but not yet typical of JBVD. Neuroradiologic findings combined with the clinical picture, ultrastructural findings, and abnormal ERG make an early diagnosis easier before the appearance of the other characteristic neurophysiologic signs [9]. Even the combination of typical MRI and clinical findings suggests JBVD.

When the CT findings in JBVD disease and JNCL are compared, it is evident that changes appear much later in JNCL; in JNCL there are no changes before 9 years of age [20]. Infratentorial atrophy also appears earlier and is more pronounced in JBVD than in JNCL [9,20].

Machen et al. [15] and Boustany et al. [21] reported the MRI findings in 9 NCL patients, 7 of whom had JNCL. Machen et al. found hyperintense periventricular white matter in the two most severely affected patients (both age 20 years). In all of our JBVD patients hyperintense periventricular white matter was found between the ages of 6-11 years. White matter changes appeared to be much earlier in JBVD than in JNCL.

On CT, JBVD is quite different from INCL, in which the atrophy is more severe and generalized and appears earlier [20,21]. Intensity changes also appear earlier and are more severe and generalized in INCL than in JBVD.

The clinical picture and lack of systemic symptoms and signs differentiate JBVD from other progressive encephalopathies that have an onset between 4 and 7 years of age [22,23]. This difference is further supported by typical MRI findings; prominent cerebellar atrophy can also be observed on CT and SPECT.

The most important pathologic finding in the classic type of Jansky-Bielschowsky disease is the variable atrophy in the cerebellum [1,2]. No detailed neuropathologic reports of JBVD are available in the literature; no explanation for the hypointensity of the thalami and putamina or for the hyperintensity periventricular white matter on MRI has been demonstrated. The decreased signal intensity in the basal ganglia and thalami in T_2-weighted images is generally believed to be due to increased iron deposition, perhaps as a nonspecific response to degeneration and decreased neurotransmitter synthesis. One explanation for the hypointense areas could be the accumulation of iron [24,25]. This accumulation is probably connected with the intracellular storage of lipofuscin in the nerve cells in NCL disorders [26,27]. Conversely, Chen et al. maintained that T_2 values on MRI correlated poorly with iron and ferritin found in neurologically intact brain [28]; however, they did not suggest that there is no correlation between iron concentration and signal intensity at higher levels of tissue iron, levels that may be found in the diseased brain. The hyperintense white matter areas may be related to diffuse demyelination, marked gliosis, and axon preservation [26].

Radiologic examinations of the brain are valuable in the early diagnosis of JBVD. They demonstrate atrophic changes that are most prominent in the posterior fossa. MRI also demonstrates parenchymal abnormalities that may be found a few months after the initial symptoms. MRI, particularly when combined with a typical clinical picture, suggests a diagnosis of JBVD. In addition to its value in the differential diagnosis, MRI may prove to be important in following the progression, as well as in investigating the pathophysiology, of the disease.

We thank Päivi Nikkinen for her valuable assistance in performing SPECT. This study was supported by the Finnish Lions Club Association.

References

[1] **Jansky** J. Dosud nepopsany pripad familiarni amauroticke idiotie komplikovane s hypoplasii mozeckovou. Sb Lék 1908;13: 165-96.

[2] **Bielschowsky** M. Über spät-infantile familiäre amaurotische idiotie mit Kleinhirnsymptomen. Dtsch Z Nervenheilkd 1913;50:7-29.

[3] **Zeman** W, Dyken P. Neuronal ceroid-lipofuscinosis (Batten's disease: Relationship to amaurotic family idiocy? Pediatrics 1969;44: 570-83.

[4] **Palmer** DN, Martinus RD, Cooper SM, Midwinter GG, Reid JC, Jolly RD. Ovine ceroid-lipofuscinosis: The major lipopigment protein and the lipid binding subunit of mitochondrial ATP synthase have the same NH2-terminal sequence. J Biol Chem 1989;264:5736-40.

[5] **Jolly** RD, Martinus RD, Shimada A, Fearnley IM, Palmer DN. Ovine ceroidlipofuscinosis is a proteolipid proteinosis. Can J Vet Res 1990;54:15-21.

[6] **Warburg** M. The natural history of Jansky-Bielschowsky's and Batten's disease. In: Armstrong D, Koppang N, Rider A, eds. Ceroid-lipofuscinoses (Batten's disease). Amsterdam: Elsevier, 1982;35-44.

[7] **Rider** JA, Rider DL. Batten disease: Past, present, and future. Am J Med Genet 1988;5(Suppl):21-6.

[8] **Santavuori** P, Rapola J, Sainio K, Raitta C. A variant of Jansky-Bielschowsky disease. Neuropediatrics 1982;13:135-41.

[9] **Santavuori** P, Rapola J, Nuutila A, et al. The spectrum of Jansky-Bielschowsky disease. Neuropediatrics 1991;22:92-6.

[10] **Dyken** PR. Reconsideration of the classification of the neuronal ceroid-lipofuscinoses. Am J Med Genet 1988;5(Suppl):69-84.

[11] **Pampiglione** G, Harden A. Neurophysiological identification of a late infantile form of "neuronal lipidosis." J Neurol Neurosurg Psychiatry 1973;36:68-74.

[12] **Valavanis** A, Friede RL, Schubiger O, Hayek J. Computed tomography in neuronal ceroid lipofuscinosis. Neuroradiology 1980;19: 35-8.

[13] **Dunn** DW. CT in ceroid lipofuscinosis. Neurology 1987;37: 1025-6.

[14] **Savolaine** ER, Voeller K, Gunning W, Smith RR. Computed tomography in neuronal ceroid lipofuscinosis: Four case reports. J Comput Tomogr 1987;11:73-8.

[15] **Machen** BC, Williams JP, Lum GB, et al. Magnetic resonance imaging in neuronal ceroid lipofuscinosis. CT J Comput Tomogr 1987; 11:160-6.

[16] **Boustany** RMN, Kolodny EH. Neurological progress the neuronal ceroid lipofuscinoses: A review. Rev Neurol 1989;145:105-10.

[17] **Edwards** MK, Bonnin JM. White matter disease. In: Atlas SW, ed. Magnetic resonance imaging of the brain and spine. New York: Raven Press, 1991;467-99.

[18] **Braffman** BH, Trojanowski JQ, Atlas SW. The aging brain and neurodegenerative disorder. In: Atlas SW, ed. Magnetic resonance imaging of the brain and spine. New York: Raven Press, 1991;567-624.

[19] **Edwards** MK. Metabolic, endocrine and iatrogenic lesions of the brain. In: Cohen MD, Edwards MK, eds. Magnetic resonance imaging of children. Philadelphia: BC Decker, 1990;305-24.

[20] **Ralninko** R, Santavuori P, Heiskala H, Sainio K, Palo J. CT findings in neuronal ceroid lipofuscinosis. Neuropediatrics 1990;21: 95-101.

[21] **Boustany** RMN, Alroy J, Kolodny EH. Clinical classification of neuronal ceroid-lipofuscinosis subtypes. Am J Med Genet 1988; 5(Suppl):47-58.

[22] **Percy** AK. The inherited neurodegenerative disorders of childhood: Clinical assessment. J Child Neurol 1987;2:82-8.

[23] **Swaiman** KF. Lysosomal diseases. In: Swaiman KF, ed. Pediatric neurology: Principles and practice. St. Louis: CV Mosby, 1989; 1017-66.

[24] **Drayer** B, Burger P, Darwin R, Riederer S, Herfkens R, Johnson GA. Magnetic resonance imaging of brain iron. AJNR 1986;7: 373-80.

[25] **Drayer** B. Imaging of the aging brain. Radiology 1988;166: 785-96.

[26] **Zeman** W, Donohue S, Dyken P, Green J. The neuronal ceroid-lipofuscinoses (Batten-Vogt syndrome). In: Vinken P, Bruyn GW, eds. Handbook of clinical neurology: Leukodystrophies and poliodystrophies. Amsterdam: North Holland, 1970;588-679.

[27] **Gutteridge** JMC, Westermarck T, Santavuori P. Iron and oxygen radicals in tissue damage: Implications for the neuronal ceroid lipofuscinosis. Lancet 1983;2:459-60.

[28] **Chen** JC, Hardy PA, Clauberg M, et al. T2 values in the human brain: Comparison with quantitative assays of iron and ferritin. Radiology 1989;173:521-2.